# 1

# Asteroseismology of red giant stars

### Rafael A. García<sup>1</sup> & Dennis Stello<sup>2</sup>

 Laboratoire AIM, CEA/DSM – CNRS - Univ. Paris Diderot – IRFU/SAp, Centre de Saclay, 91191 Gif-sur-Yvette Cedex, France
Sydney Institute for Astronomy (SIfA), School of Physics, University of Sydney, NSW 2006, Australia

#### 1.1 Introduction

If appropriately excited, a star will oscillate like a giant spherical instrument. In most stars, including the Sun, surface convection provides the excitation mechanism (Goldreich and Keeley, 1977). With turbulent velocities reaching speeds comparable to the local sound speed near the surface of the star, the vigorous convective motions can excite standing acoustic waves. These are known as pressure or p modes because the restoring force arises from the pressure gradient. The broad frequency spectrum of this excitation mechanism gives rise to many oscillation modes, both radial and non-radial, excited simultaneously. These stochastically excited and intrinsically damped oscillations were first detected in the Sun (Leighton et al., 1962), and hence are commonly known as solar-like oscillations.

Oscillation modes can be characterised by the number of nodes, n, in the radial direction, called the radial order, and a non-radial part described by spherical harmonics, each with an angular degree, l, which equals the number of nodal lines on the surface, and an azimuthal order, m, which is the number of those nodal lines crossing the equator of the star. Except for the Sun, we can genrally not resolve these oscillations on the surfaces of cool stars and so the surface displacements of modes with high angular degree ( $l \gtrsim 4$ ) cannot be observed because regions of opposite phase tend to cancel out.

When stars grow old and the supply of hydrogen fuel is exhausted in the core, their envelopes expand and cool: they become subgiants and eventually red giants. This transition is shown in the so-called HR-diagram in Fig 1.1, which indicates the main stages of evolution of a one solar mass star from the 'main sequence' where the Sun is currently located (between points 1-2) through to the red giant phase discussed in this chapter (beyond point 3). Like the Sun, red giants have convective outer envelopes but the much longer convective

time scales drives oscillation modes at much lower frequencies. The expansion and contraction of different parts of the stellar surface when a star oscillates gives rise to variations in temperature – and hence also luminosity – across the stellar surface. For the Sun, the surface moves with about walking speed and has an oscillation amplitude of the order of 100 m. The corresponding brightness variations are only of a few parts per million (ppm), equivalent to temperature fluctuations of about 0.1 K. In most red giants, those brightness variations have increased to several tens, even hundreds of ppm, which is however, still relatively small compared to the twinkling of stars we see at night caused by the Earth's atmosphere. From the ground, the most successful method for detecting the oscillations has therefore been using time-series spectroscopy to detect the surface velocity changes, through the Doppler shift of the light, as the stellar surface moves in and out. This method is not impacted by the twinkling of stars but current limitations on the ultra high-precision spectrographs required for these observations generally restrict investigations to one target at a time. Hence, to do large scale investigations one needs to use photometry to measure the brightness of many stars all at the same time, which requires space-based observations.

Before asteroseismology entered the space age, a range of ground-based efforts were carried out using either spectroscopy or photometry. Measurements of solar-like oscillations were pursued since the early 1990s (e.g. Gilliland et al., 1993, and references herein), but it was nearly a decade later before we saw the first firm detection in a red giant (Frandsen et al., 2002). Despite an increasing number of oscillating red giants detected from ground (e.g. Barban et al., 2004; De Ridder et al., 2006) and early space missions (Buzasi et al., 2000; Retter et al., 2003; Barban et al., 2007; Gilliland, 2008), at the time, it was still not clear whether these stars showed both radial and non-radial modes (Christensen-Dalsgaard, 2004), and hence how strong the mode damping was (Stello et al., 2006). It was therefore not known how information rich and useful red giants would be as seismic targets. In an ambitious attempt to detect oscillations in a large group of red giants in the open cluster M67 using 10 telescopes simultaneously for over one month, only marginal detections were achieved, which concluded almost two decades of ground-based photometric attempts (Stello et al., 2007).

#### 1.2 Red giants: the new frontier in asteroseismology

It was data from space missions that transformed the field and demonstrated that red giants show rich spectra of oscillation frequencies. The existence of non-radial modes (see Fig. 1.2) were indicated in a few bright stars observed by the star tracker camera on the WIRE spacecraft (Stello et al., 2008). But it was a sample of hundreds of stars observed by CoRoT that unambiguously demonstrated that red giants exhibit both radial and non-radial modes (De Ridder et al., 2009). Shortly after this came the initial results from the Kepler Mission, which provided more precise data for even larger numbers of stars (Gilliland et al., 2010; Bedding et al., 2010), confirming they pulsate with both radial and non-radial modes, whose frequency patterns resembled that of the roughly equally-spaced acoustic

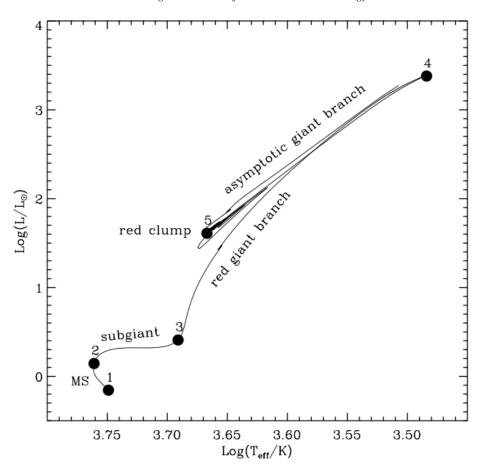


Figure 1.1 HR diagram of a stellar model for a one solar mass star of solar composition, showing luminosity in solar units versus effective (surface) temperature. The star starts its life burning hydrogen at the zero-age-main-sequence (point 1). Each following evolution phase is indicated as follows: 1-2: main sequence (hydrogen core burning); 2-3: subgiant (hydrogen shell burning); 3-4: red giant branch (hydrogen shell burning); 4: red giant branch tip (helium ignition); 5: red clump (helium core burning); 5 and up: asymptotic giant branch (helium shell burning).

modes in the Sun, but at lower frequencies. However, in a few percent of stars the dipole modes showed unexplained low amplitudes (Mosser et al., 2012a; García et al., 2014). Over a period of only 2-3 years, the number of red giants with detected oscillations went from a handful (pre-CoRoT) into the thousands (Mosser et al., 2010; Kallinger et al., 2010; Hekker et al., 2011; Huber et al., 2011; Miglio et al., 2012b; Stello et al., 2013). These long high-precision time series for large numbers of stars opened up a completely new way of exploring red giants using asteroseismology.

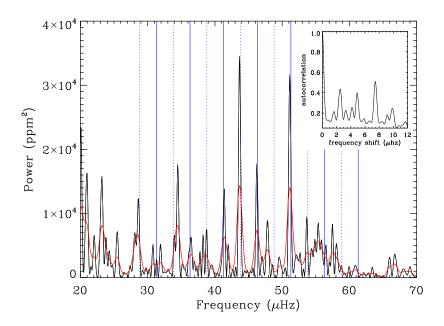


Figure 1.2 Power spectrum of the red giant  $\beta$ Vol observed by the star tracker on the *WIRE* spacecraft (smoothed version in red). Equally spaced vertical solid and dotted lines indicate radial and dipole modes, respectively. The inset shows the autocorrelation of the spectrum, showing peaks at multiples of half of the large frequency spacing:  $\Delta\nu/2$  (Stellar Pulsation and Evolution 2007, Vancouver).

The large frequency separation computed from the equally-spaced overtone modes provide information on the density of the star. Through scaling relations anchored at the solar values, this information combined with the frequency of maximum power,  $\nu_{\rm max}$ , and the effective temperature allows estimation of mass and radius for stars pulsating from minutes to hundreds of days (See Fig. 1.3). These relations have been extensively tested for both main-sequence and red giant stars with additional constraints such as parallax measurements or individual frequencies (Stello et al., 2008; Bedding, 2011; Miglio et al., 2012a; Mathur et al., 2012) and by using stellar models (Stello et al., 2009; White et al., 2011; Miglio et al., 2013a; Belkacem et al., 2013). Recent independent methods have verified the scaling relations at the 4–5% level (Huber et al., 2011; White et al., 2013; Silva Aguirre et al., 2012), although uncertainties remain about additional systematics for giants at certain stages of their evolution, which need further investigation (Miglio et al., 2012a, 2013a). Masses and radii can therefore be inferred for a wide range of evolutionary stages from the main sequence through to the red giant branch, the clump, and even asymptotic giant branch stars (Corsaro et al., 2012).

Among the most luminous red giants observed by *Kepler*, it was showed that also they pulsate in both radial and non-radial modes (Mosser et al., 2013), concluding a decade-long

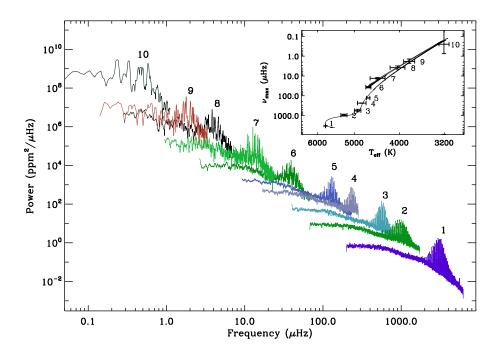


Figure 1.3 Sequence of stellar oscillation spectra starting from a main sequence star, the Sun (#1), to the tip of the red giant branch. Star #6 is a red clump star. Temperatures are from the *Kepler* Input Catalog (Brown et al., 2011) and from Huber et al. (2014). The inset represents a seismic HR diagram. The solid line is the evolutionary track of a one solar-mass stellar model computed using MESA (Paxton et al., 2011, 2013) in which the position of each star is represented. The 1- $\sigma$  error bars in  $\nu_{\rm max}$  are multiplied by a factor of 10.

debate about the possible presence of non-radial modes in these highly evolved stars. Stello et al. 2014[REF IN BIB] further demonstrated that the frequency pattern of these stars was markedly different from that of lesser evolved stars with dipole modes dominating the power frequency spectrum and being shifted relative to the radial modes.

#### 1.3 Mixed modes: a window into the inner radiative core of red giants

One of the key reasons red giants have been such a success story reaching even beyond the field of asteroseismology in recent years is the presence of so called mixed modes, predicted by Dupret et al. (2009) and later observed by Bedding et al. (2010). In the following, we will explain how these modes occur. The stellar interior of cool stars essentially consists of two cavities, an outer envelope where standing acoustic waves (p modes) predominantly reside, and a radiative core where standing gravity waves (g modes) propagate.

For a star like the Sun, p-mode frequencies are much higher than those of the g modes – 3000  $\mu$ Hz or 5 minutes compared to 100  $\mu$ Hz or 2.8 hours, respectively. They therefore do not 'sense' the presence of each other. When a star evolves to become a red giant the core contraction and the envelope expansion results in the p-mode frequencies becoming lower while the g-mode frequencies become higher and eventually resulting in overlapping p- and g-mode frequencies. This causes the two types of waves to couple. When a p mode couples with a g mode and form a mixed mode its frequency is shifted – the mode is bumped from its original position - as the two modes undergo a so-called 'avoided crossing'. The regular frequency spacing between consecutive modes of the same degree and different order is broken. The first mixed modes occur during the subgiant phase where the associated mode bumping can be observed. Examples include stars like  $\eta$  Boo (Kjeldsen et al., 1995; Carrier et al., 2005),  $\beta$  Hyi (Bedding et al., 2007; Belloche et al., 2011), the CoRoT subgiant HD 49385 (Deheuvels et al., 2010), and many Kepler targets (e.g. Mathur et al., 2011, 2012; Campante et al., 2011). An example, based on the Kepler target KIC 11026764 (Metcalfe et al., 2010), is shown in Fig. 1.4. The left-hand panel shows the temporal evolution of radial and dipole modes of a series of models. Each instance where the dipole p mode (solid line) moves up in time, we have an avoided crossing with an underlying g mode whose presence can be traced by the series of mode bumpings of ever increasing frequency. The model that best matches the observations is marked with a vertical line. The corresponding échelle diagram is showed in the right-hand panel, which is expected to show near vertical ridges for modes of the same spherical degree l, meaning almost equidistant frequencies following the typical pattern of high-order low-degree acoustic modes described by the asymptotic relation (REF TASSOUL). Bumped dipole modes are clearly seen around 900  $\mu$ Hz, revealing the presence of a g mode at that frequency.

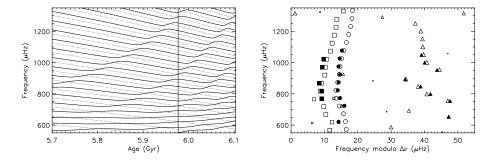


Figure 1.4 Left: Temporal evolution of the l=0 (dotted) and l=1 (solid) oscillation frequencies based on KIC 11026764 (Metcalfe et al., 2010). The vertical solid line indicates the location of the model whose frequencies matches the observed. Right: Échelle diagram using a frequency separation of  $\Delta \nu = 50.5~\mu Hz$ . Open symbols are the frequencies from the best fitting model. Solid symbols are the observed frequencies from Metcalfe et al. (2010). Circles are used for modes with l=0, triangles for l=1, and squares for l=2 modes (Figure courtesy of Dr. G. Doğan).

When stars reach the red giant phase, the frequency spectrum of the g modes become denser than that of the p-modes. Hence, for each p mode there are several g modes with the same angular degree and similar frequencies, each coupling to the p mode leading to several mixed modes with a p mode character in the envelope and a g mode character in the core (Osaki, 1975; Aizenman et al., 1977; Dziembowski and Pamyatnykh, 1991; Beck et al., 2011). Because of the coupling, mixed modes carry valuable information about the inner radiative interior directly to the surface, and due to their p-mode character, their amplitudes are high enough to be detected at the surface. This is in contrast to main sequence stars like the Sun where g modes reach the stellar surface with tiny amplitudes because these modes are evanescent in the convective envelope, making them difficult to detect (García et al., 2007).

The closer in frequency a g mode is to a p mode the more p-mode dominated the resulting mixed modes will be. A series of g modes coupling to the same p mode therefore generates mixed modes with different degree of p- and g-mode character, each probing different regions of the stellar interior, allowing a stratified 'view' of the stellar interior.

#### 1.4 Period spacings: a way to distinguish different stellar evolution phases

Classical observations of the surface properties of red giants do not allow us to disentangle stars ascending the red giant branch – only burning hydrogen in a shell – from stars in later evolution stages also burning helium in their cores such as the red clump stars (Fig ??).

By measuring the period spacing of the dipole mixed modes, Bedding et al. (2011) realized that red giants fall into two well defined groups, those with period spacings around 50 seconds (hydrogen-shell-burning stars) and those with period spacings ranging between 100 to 300 seconds (stars also burning helium in the core). The reason for this divide arise because g modes senses the difference in the core as it becomes convective and expands due to the onset of the helium burning. Kallinger et al. (2012) demonstrated that the constant term of a linear fit to the radial modes versus their radial order also enabled them to characterise this divide.

This characterisation can now be done automatically for very large samples of stars. In Fig. 1.5 we show the period spacing,  $\Delta P$ , against the large frequency separation of several thousand red giant stars observed by *Kepler* (Stello et al., 2013). Red giant branch stars have period spacings below  $\sim 80$  s. Red clump stars are mostly concentrated above 180 s, being the less massive stars clustering on the left-hand side of the diagram (lower  $\Delta \nu$ ), when they reach this evolutionary stage. The more massive helium-core-burning stars in the clump form the high- $\Delta \nu$  low- $\Delta P$  tail of the helium core burning stars (marked  $2^{\rm nd}RC$ ).

In Fig. 1.6 we show the power spectrum around the frequency of maximum power,  $\nu_{\rm max}$ , of two red giants observed during  $\sim$ 4 years by *Kepler*, one on the red giant branch and the other in the red clump (for more details see Kallinger et al., 2012). The red clump star shows a relatively large spacing between consecutive dipole modes (large  $\Delta P$ ) while the red giant branch star has its dipole modes bunched closely together (small  $\Delta P$ ).

It was further noted by Montalbán et al. (2013) that  $\Delta P$  to some degree follows the

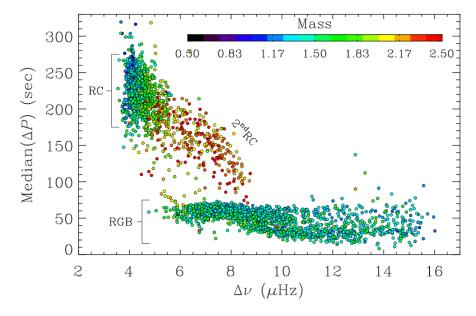


Figure 1.5 Median period spacing of mixed modes for each star analyzed by Stello et al. (2013) versus its large frequency separation. Red giant branch (RGB), red clump (RC), and secondary clump (2<sup>nd</sup>RC) stars are indicated. The mass of the stars obtained from the scaling relations are color coded.

helium core mass for stars that has just ignited helium in their cores. This potentially gives a way to measure the amount of mixing that took place in these stars during their earlier evolution stages.

## 1.5 Differential rotation inside red giants

Mixed modes not only allow us to extract the structure of the inner core of red giants, they also probe the distribution of internal angular momentum during the evolution along the red giant branch. Information about the angular momentum distribution is inaccessible to direct observations, but it can be inferred from the effect of rotation on oscillation frequencies. An extensive overview on surface and internal rotation of stars can be found in chapter 5.6. Here we will give only a brief explanation of the most important discoveries related to red giants.

Beck et al. (2012) detected non-rigid rotation in the interior of three *Kepler* red giants by exploiting the rotational frequency splitting of mixed modes. An example of the power spectrum of one of these stars, KIC 5356201, can be seen in Fig.1.7. Deheuvels et al. (2012) performed an inversion of the radial rotation profile in an early red giant, KIC 7341231, and recently Deheuvels et al. (2014) analysed the rotation of six subgiants and red giants within a range of metallicities and masses. The latter study demonstrated that the stellar

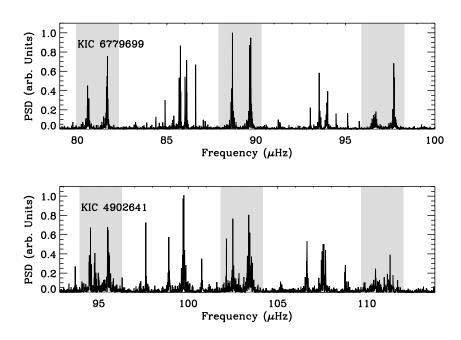


Figure 1.6 Normalized power spectral density (PSD) of two red giant stars, one on the red giant branch (top) and the other in the red clump (bottom). Shaded regions correspond to the l=0,2 modes, while the unshaded regions are dominated by dipole mixed modes.

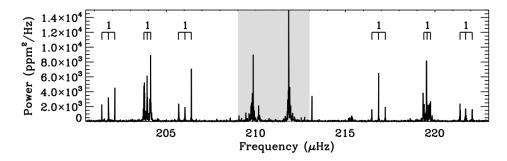


Figure 1.7 Power density spectrum of KIC 5356201 observed during nearly 4 years by *Kepler*. Rotationally split l=1 mixed modes are marked. The shaded regions covers the l=0,2 modes.

cores spun up during the subgiant phase, while the envelopes spun down. For two of the stars, the radial rotation profile showed a discontinuity located at the depth of the hydrogen-

burning shell, which roughly corresponds to the boundary between the contracting and the expanding layers.

The ensemble analysis of around 300 red giants (see the next section for more details on ensemble studies), performed by Mosser et al. (2012b) showed the evolution of the rotation rate of the radiative cores from the subgiant phase to the red clump and the 2<sup>nd</sup>RC. It demonstrated that the rotational splitting of dipole mixed modes is mostly sensitive to the core rotation (Goupil et al., 2013). In the earlier stages of the red giant branch, the core rotation shows a slight decrease as the stars evolve. This seems to be in contradiction with core contraction when only local conservation of angular momentum is assumed (e.g. Eggenberger et al., 2012; Ceillier et al., 2013; Marques et al., 2013). Later, when stars reach the red clump, the cores have spun down even more. Part of this effect is related to the expansion of the helium burning core (Iben, 1971; Sills and Pinsonneault, 2000). Nevertheless, this spin down of the core during the red giant branch and to the red clump seems to be in agreement with the slow rotation rate found in low-mass white dwarfs (Kawaler et al., 1999), which are essentially the end product of red giant cores after the envelope has been stripped away during the late stages of red giants.

#### 1.6 Ensemble Asteroseismology and Stellar populations

With more than 16,000 red giants observed by *Kepler* and about the same number observed by CoRoT, the space age of asteroseismology has opened up for the statistical analysis of large samples of stars usually called 'ensemble asteroseismology'. Helped by these large numbers, we can identify new and common features in asteroseismic diagrams revealing key properties of stellar evolution, while providing ideal tracers of Galactic stellar evolution history to relative large distances (Miglio et al., 2009).

Using the scaling relations for  $\Delta\nu$  and  $\nu_{\rm max}$  (Kjeldsen and Bedding, 1995) on ensembles can provide valuable results on the mass and radius distributions of large cohorts of stars. Aided by stellar modeling, such ensemble analysis can also provide estimates of the age distributions. When combining radius with the apparent stellar brightness we can further estimate distances out to several kiloparsecs (1 parsec  $\sim$  3 light years). In comparison, precise distances currently available from direct parallax measurements (van Leeuwen, 2007) reach only a few hundred parces. Hence, for red giants or any other solar-like oscillating star it is possible to write:

$$\log d = 1 + 2.5 \log \frac{T_{\text{eff}}}{T_{\text{eff},\odot}} + \log \frac{\nu_{\text{max}}}{\nu_{\text{max},\odot}} - 2 \log \frac{\Delta \nu}{\Delta \nu_{\odot}} + 0.2 (m_{\text{bol}} - M_{\text{bol},\odot}), \quad (1.1)$$

where the distance d is expressed in parsecs,  $m_{\rm bol}$  is the apparent stellar bolometric magnitude, and  $M_{\rm bol,\odot}$  is the absolute solar bolometric magnitude,  $T_{\rm eff}$  is the effective (surface) temperature, and  $\odot$  denotes the solar values (Miglio et al., 2013b). Therefore, it is possible to use red giants to map and date the Galactic disc in the regions probed by space-borne missions such as CoRoT and Kepler, and in the future TESS (Ricker et al., 2010) and PLATO (Rauer et al., 2013). The results from CoRoT and Kepler compared to models of

synthetic populations of stars already revealed significant differences in the stellar mass distributions. One interpretation of these results explains this as due to the vertical gradient in the distribution of stellar masses (hence ages) in the galactic disk (Miglio et al., 2013b), as well as on the star-formation rate, and the initial mass function of stars (Miglio et al., 2009; Chaplin et al., 2011).

Another important contributor to galactic evolution is the rate of mass-loss when the stars evolve as red giants. There is currently no adequate physical theory on the mass loss occurring at late stages of the red giant branch that can properly explain observations. Ensemble asteroseismology can provide important information on this crucial phase of stellar evolution by comparing the mass distribution of red clump stars with stars on the red giant branch (see next section). Using CoRoT and *Kepler* observations, it has been shown that there is a population of low-mass red clump stars which is absent on the red giant branch (Mosser et al., 2011). Assuming the scaling relations used to infer those masses are not introducing any systematic effects of such sort, this result could imply that these now low-mass red clump stars lost a significant fraction of their mass while ascending on the red giant branch. Therefore, after the helium flash, these stars appear in the red clump with a much lower mass than the one they had during the red giant branch.

#### 1.7 Asteroseismology of open-cluster red giants

Open clusters have long served as universal calibrators in astronomy because stars in a cluster are considered a homogeneous sample. They are supposed to be formed from the same cloud of gas, which means they have roughly the same age, common initial composition, and are at the same distance. In stellar physics, these assumptions reduce the number of usual unknowns when matching stellar models to observations, which in combination with precise asteroseismic measurements promises more rigorous investigation of stellar models.

The scaling relations for  $\Delta\nu$  and  $\nu_{\rm max}$  mentioned in sections 1.2 and 1.6 allows us to assign membership of stars to a particular cluster. The relations depend on stellar mass, surface temperature, and luminosity, but only the latter will be markedly different from star to star among red giants in a cluster. Hence,  $\Delta\nu$  and  $\nu_{\rm max}$  are expected to form tight relations with apparent brigness, which for cluster members is a good proxy for luminosity, and outliers are therefore likely non-members due to them not sharing the cluster distance. Because oscillations only depend on the stellar properties, this technique is independent of the distance to the cluster and not very sensitive to the interstellar absorption and reddening (Stello et al., 2011). Another important success of asteroseismology of open clusters was the determination of the distances to NGC 6791 and NGC 6819 based on the seismic studies of red giant branch stars using grid-based modeling (Basu et al., 2011). Finally, Miglio et al. (2012a) estimated the integrated red giant branch mass loss in NGC 6791 by comparing the average masses of stars in the red clump and on the red giant branch.

- Aizenman, M., Smeyers, P., and Weigert, A. 1977. Avoided Crossing of Modes of Non-radial Stellar Oscillations. A&A, **58**(June), 41.
- Barban, C., De Ridder, J., Mazumdar, A., et al. 2004 (Oct.). Detection of Solar-Like Oscillations in Two Red Giant Stars. Page 113 of: Danesy, D. (ed), *SOHO 14 Helio-and Asteroseismology: Towards a Golden Future*. ESA Special Publication, vol. 559.
- Barban, C., Matthews, J. M., De Ridder, J., et al. 2007. Detection of solar-like oscillations in the red giant star  $\epsilon$  Ophiuchi by MOST spacebased photometry. A&A, **468**(June), 1033–1038.
- Basu, S., Grundahl, F., Stello, D., et al. 2011. Sounding Open Clusters: Asteroseismic Constraints from Kepler on the Properties of NGC6791 and NGC6819. ApJ, **729**(Mar.), L10.
- Beck, P. G., Bedding, T. R., Mosser, B., et al. 2011. Kepler Detected Gravity-Mode Period Spacings in a Red Giant Star. *Science*, **332**(Apr.), 205.
- Beck, P. G., Montalban, J., Kallinger, T., et al. 2012. Fast core rotation in red-giant stars as revealed by gravity-dominated mixed modes. Nature, **481**(Jan.), 55–57.
- Bedding, T. R. 2011. Solar-like Oscillations: An Observational Perspective. *arXiv:1107.1723*, July.
- Bedding, T. R., Kjeldsen, H., Arentoft, T., et al. 2007. Solar-like Oscillations in the G2 Subgiant β Hydri from Dual-Site Observations. ApJ, **663**(July), 1315–1324.
- Bedding, T. R., Huber, D., Stello, D., et al. 2010. Solar-like Oscillations in Low-luminosity Red Giants: First Results from Kepler. ApJ, **713**(Apr.), L176–L181.
- Bedding, T. R., Mosser, B., Huber, D., et al. 2011. Gravity modes as a way to distinguish between hydrogen- and helium-burning red giant stars. Nature, **471**(Mar.), 608–611.
- Belkacem, K., Samadi, R., Mosser, B., Goupil, M.-J., and Ludwig, H.-G. 2013 (Dec.). On the Seismic Scaling Relations Delta nu rho and nu max nu c. Page 61 of: Shibahashi, H., and Lynas-Gray, A. E. (eds), *Astronomical Society of the Pacific Conference Series*. Astronomical Society of the Pacific Conference Series, vol. 479.
- Belloche, A., Schuller, F., Parise, B., et al. 2011. The end of star formation in Chamaeleon I?. A LABOCA census of starless and protostellar cores. A&A, **527**(Mar.), A145.
- Brown, T. M., Latham, D. W., Everett, M. E., and Esquerdo, G. A. 2011. Kepler Input Catalog: Photometric Calibration and Stellar Classification. AJ, **142**(Oct.), 112.
- Buzasi, D., Catanzarite, J., Laher, R., et al. 2000. The Detection of Multimodal Oscillations on  $\alpha$  Ursae Majoris. ApJ, **532**(Apr.), L133–L136.
- Campante, T. L., Handberg, R., Mathur, S., et al. 2011. Asteroseismology from multimonth Kepler photometry: the evolved Sun-like stars KIC 10273246 and KIC 10920273. A&A, **534**(Oct.), A6.

- Carrier, F., Eggenberger, P., and Bouchy, F. 2005. New seismological results on the G0 IV  $\eta$  Bootis. A&A, **434**(May), 1085–1095.
- Ceillier, T., Eggenberger, P., García, R. A., and Mathis, S. 2013. Understanding angular momentum transport in red giants: the case of KIC 7341231. A&A, 555(July), A54.
- Chaplin, W. J., Kjeldsen, H., Christensen-Dalsgaard, J., et al. 2011. Ensemble Asteroseismology of Solar-Type Stars with the NASA Kepler Mission. *Science*, **332**(Apr.), 213–.
- Christensen-Dalsgaard, J. 2004. Physics of solar-like oscillations. Sol. Phys., **220**(Apr.), 137–168.
- Corsaro, E., Stello, D., Huber, D., et al. 2012. Asteroseismology of the Open Clusters NGC 6791, NGC 6811, and NGC 6819 from 19 Months of Kepler Photometry. ApJ, 757(Oct.), 190.
- De Ridder, J., Barban, C., Carrier, F., et al. 2006. Discovery of solar-like oscillations in the red giant \varepsilon Ophiuchi. A&A, **448**(Mar.), 689–695.
- De Ridder, J., Barban, C., Baudin, F., et al. 2009. Non-radial oscillation modes with long lifetimes in giant stars. Nature, **459**(May), 398–400.
- Deheuvels, S., Bruntt, H., Michel, E., et al. 2010. Seismic and spectroscopic characterization of the solar-like pulsating CoRoT target HD 49385. A&A, **515**(June), A87.
- Deheuvels, S., García, R. A., Chaplin, W. J., et al. 2012. Seismic Evidence for a Rapidly Rotating Core in a Lower-giant-branch Star Observed with Kepler. ApJ, **756**(Sept.), 19.
- Deheuvels, S., Doğan, G., Goupil, M. J., et al. 2014. Seismic constraints on the radial dependence of the internal rotation profiles of six Kepler subgiants and young red giants. *ArXiv e-prints*, Jan.
- Dupret, M.-A., Belkacem, K., Samadi, R., et al. 2009. Theoretical amplitudes and lifetimes of non-radial solar-like oscillations in red giants. A&A, **506**(Oct.), 57–67.
- Dziembowski, W. A., and Pamyatnykh, A. A. 1991. A potential asteroseismological test for convective overshooting theories. A&A, **248**(Aug.), L11–L14.
- Eggenberger, P., Montalbán, J., and Miglio, A. 2012. Angular momentum transport in stellar interiors constrained by rotational splittings of mixed modes in red giants. A&A, **544**(Aug.), L4.
- Frandsen, S., Carrier, F., Aerts, C., et al. 2002. Detection of Solar-like oscillations in the G7 giant star xi Hya. A&A, **394**(Oct.), L5–L8.
- García, R. A., Turck-Chièze, S., Jiménez-Reyes, S. J., et al. 2007. Tracking Solar Gravity Modes: The Dynamics of the Solar Core. *Science*, **316**(June), 1591–1593.
- García, R. A., Pérez Hernández, F., Benomar, O., et al. 2014. Study of KIC 8561221 observed by Kepler: an early red giant showing depressed dipolar modes. A&A, 563(Mar.), A84.
- Gilliland, R. L. 2008. Photometric Oscillations of Low-Luminosity Red Giant Stars. AJ, **136**(Aug.), 566–579.
- Gilliland, R. L., Brown, T. M., Kjeldsen, H., et al. 1993. A search for solar-like oscillations in the stars of M67 with CCD ensemble photometry on a network of 4 M telescopes. AJ, **106**(Dec.), 2441–2476.
- Gilliland, R. L., Brown, T. M., Christensen-Dalsgaard, J., et al. 2010. Kepler Asteroseis-mology Program: Introduction and First Results. PASP, **122**(Feb.), 131–143.
- Goldreich, P., and Keeley, D. A. 1977. Solar seismology. II The stochastic excitation of the solar p-modes by turbulent convection. ApJ, **212**(Feb.), 243–251.

- Goupil, M. J., Mosser, B., Marques, J. P., et al. 2013. Seismic diagnostics for transport of angular momentum in stars. II. Interpreting observed rotational splittings of slowly rotating red giant stars. A&A, **549**(Jan.), A75.
- Hekker, S., Gilliland, R. L., Elsworth, Y., et al. 2011. Characterization of red giant stars in the public Kepler data. MNRAS, **414**(July), 2594–2601.
- Huber, D., Bedding, T. R., Stello, D., et al. 2011. Testing Scaling Relations for Solar-like Oscillations from the Main Sequence to Red Giants Using Kepler Data. ApJ, 743(Dec.), 143.
- Huber, D., Silva Aguirre, V., Matthews, J. M., et al. 2014. Revised Stellar Properties of Kepler Targets for the Quarter 1-16 Transit Detection Run. ApJS, **211**(Mar.), 2.
- Iben, Jr., I. 1971. Globular Cluster Stars: Results of Theoretical Evolution and Pulsation Studies Compared with the Observations. PASP, 83(Dec.), 697.
- Kallinger, T., Mosser, B., Hekker, S., et al. 2010. Asteroseismology of red giants from the first four months of Kepler data: Fundamental stellar parameters. A&A, 522(Nov.), A1.
- Kallinger, T., Hekker, S., Mosser, B., et al. 2012. Evolutionary influences on the structure of red-giant acoustic oscillation spectra from 600d of Kepler observations. A&A, 541(May), A51.
- Kawaler, S. D., Sekii, T., and Gough, D. 1999. Prospects for Measuring Differential Rotation in White Dwarfs through Asteroseismology. ApJ, **516**(May), 349–365.
- Kjeldsen, H., and Bedding, T. R. 1995. Amplitudes of stellar oscillations: the implications for asteroseismology. A&A, **293**(Jan.), 87–106.
- Kjeldsen, H., Bedding, T. R., Viskum, M., and Frandsen, S. 1995. Solarlike oscillations in eta Boo. AJ, **109**(Mar.), 1313–1319.
- Leighton, R. B., Noyes, R. W., and Simon, G. W. 1962. Velocity Fields in the Solar Atmosphere. I. Preliminary Report. ApJ, **135**(Mar.), 474.
- Marques, J. P., Goupil, M. J., Lebreton, Y., et al. 2013. Seismic diagnostics for transport of angular momentum in stars. I. Rotational splittings from the pre-main sequence to the red-giant branch. A&A, **549**(Jan.), A74.
- Mathur, S., Handberg, R., Campante, T. L., et al. 2011. Solar-like Oscillations in KIC 11395018 and KIC 11234888 from 8 Months of Kepler Data. ApJ, **733**(June), 95.
- Mathur, S., Metcalfe, T. S., Woitaszek, M., et al. 2012. A Uniform Asteroseismic Analysis of 22 Solar-type Stars Observed by Kepler. ApJ, **749**(Apr.), 152.
- Metcalfe, T. S., Monteiro, M. J. P. F. G., Thompson, M. J., et al. 2010. A Precise Asteroseismic Age and Radius for the Evolved Sun-like Star KIC 11026764. ApJ, **723**(Nov.), 1583–1598.
- Miglio, A., Montalbán, J., Baudin, F., et al. 2009. Probing populations of red giants in the galactic disk with CoRoT. A&A, **503**(Sept.), L21–L24.
- Miglio, A., Brogaard, K., Stello, D., et al. 2012a. Asteroseismology of old open clusters with Kepler: direct estimate of the integrated red giant branch mass-loss in NGC 6791 and 6819. MNRAS, **419**(Jan.), 2077–2088.
- Miglio, A., Morel, T., Barbieri, M., et al. 2012b. Solar-like pulsating stars as distance indicators: G-K giants in the CoRoT and Kepler fields. *Assembling the Puzzle of the Milky Way, Le Grand-Bornand, France, Edited by C. Reylé; A. Robin; M. Schultheis; EPJ Web of Conferences, Volume 19, id.05012*, **19**(Feb.), 5012.
- Miglio, A., Chiappini, C., Morel, T., et al. 2013a (Mar.). Differential population studies using asteroseismology: Solar-like oscillating giants in CoRoT fields LRc01 and LRa01. Page 3004 of: *European Physical Journal Web of Conferences*. European Physical Journal Web of Conferences, vol. 43.

- Miglio, A., Chiappini, C., Morel, T., et al. 2013b. Galactic archaeology: mapping and dating stellar populations with asteroseismology of red-giant stars. MNRAS, **429**(Feb.), 423–428.
- Montalbán, J., Miglio, A., Noels, A., et al. 2013. Testing Convective-core Overshooting Using Period Spacings of Dipole Modes in Red Giants. ApJ, **766**(Apr.), 118.
- Mosser, B., Belkacem, K., Goupil, M.-J., et al. 2010. Red-giant seismic properties analyzed with CoRoT. A&A, 517(July), A22.
- Mosser, B., Barban, C., Montalbán, J., et al. 2011. Mixed modes in red-giant stars observed with CoRoT. A&A, **532**(Aug.), A86.
- Mosser, B., Elsworth, Y., Hekker, S., et al. 2012a. Characterization of the power excess of solar-like oscillations in red giants with Kepler. A&A, **537**(Jan.), A30.
- Mosser, B., Goupil, M. J., Belkacem, K., et al. 2012b. Spin down of the core rotation in red giants. A&A, **548**(Dec.), A10.
- Mosser, B., Dziembowski, W. A., Belkacem, K., et al. 2013. Period-luminosity relations in evolved red giants explained by solar-like oscillations. A&A, **559**(Nov.), A137.
- Osaki, J. 1975. Nonradial oscillations of a 10 solar mass star in the main-sequence stage. PASJ, 27, 237–258.
- Paxton, B., Bildsten, L., Dotter, A., et al. 2011. Modules for Experiments in Stellar Astrophysics (MESA). ApJS, **192**(Jan.), 3.
- Paxton, B., Cantiello, M., Arras, P., et al. 2013. Modules for Experiments in Stellar Astrophysics (MESA): Planets, Oscillations, Rotation, and Massive Stars. ApJS, **208**(Sept.), 4.
- Rauer, H., Catala, C., Aerts, C., et al. 2013. The PLATO 2.0 Mission. *ArXiv e-prints*, Oct. Retter, A., Bedding, T. R., Buzasi, D. L., Kjeldsen, H., and Kiss, L. L. 2003. Oscillations in Arcturus from WIRE Photometry. ApJ, **591**(July), L151–L154.
- Ricker, G. R., Latham, D. W., Vanderspek, R. K., et al. 2010 (Jan.). Transiting Exoplanet Survey Satellite (TESS). Page 450.06 of: *American Astronomical Society Meeting Abstracts 215*. Bulletin of the American Astronomical Society, vol. 42.
- Sills, A., and Pinsonneault, M. H. 2000. Rotation of Horizontal-Branch Stars in Globular Clusters. ApJ, **540**(Sept.), 489–503.
- Silva Aguirre, V., Casagrande, L., Basu, S., et al. 2012. Verifying Asteroseismically Determined Parameters of Kepler Stars Using Hipparcos Parallaxes: Self-consistent Stellar Properties and Distances. ApJ, **757**(Sept.), 99.
- Stello, D., Kjeldsen, H., Bedding, T. R., and Buzasi, D. 2006. Oscillation mode lifetimes in  $\xi$  Hydrae: will strong mode damping limit asteroseismology of red giant stars? A&A, **448**(Mar.), 709–715.
- Stello, D., Bruntt, H., Kjeldsen, H., et al. 2007. Multisite campaign on the open cluster M67 - II. Evidence for solar-like oscillations in red giant stars. MNRAS, 377(May), 584–594.
- Stello, D., Bruntt, H., Preston, H., and Buzasi, D. 2008. Oscillating K Giants with the WIRE Satellite: Determination of Their Asteroseismic Masses. ApJ, **674**(Feb.), L53–L56.
- Stello, D., Chaplin, W. J., Basu, S., Elsworth, Y., and Bedding, T. R. 2009. The relation between  $\Delta\nu$  and  $\nu_{max}$  for solar-like oscillations. MNRAS, **400**(Nov.), L80–L84.
- Stello, D., Meibom, S., Gilliland, R. L., et al. 2011. An Asteroseismic Membership Study of the Red Giants in Three Open Clusters Observed by Kepler: NGC 6791, NGC 6819, and NGC 6811. ApJ, **739**(Sept.), 13.
- Stello, D., Huber, D., Bedding, T. R., et al. 2013. Asteroseismic Classification of Stellar Populations among 13,000 Red Giants Observed by Kepler. ApJ, **765**(Mar.), L41.

- van Leeuwen, F. 2007. *Hipparcos, the New Reduction of the Raw Data*. Astrophysics and Space Science Library, vol. 350.
- White, T. R., Bedding, T. R., Stello, D., et al. 2011. Calculating Asteroseismic Diagrams for Solar-like Oscillations. ApJ, **743**(Dec.), 161.
- White, T. R., Huber, D., Maestro, V., et al. 2013. Interferometric radii of bright Kepler stars with the CHARA Array: theta Cygni and 16 Cygni A and B. MNRAS, **433**(Aug.), 1262–1270.